Droplet Microscope Individual Selection Report

(Dated: April 7, 2024)

By looking through a single water droplet placed on a glass surface, one can observe that the droplet acts as an imaging system. We wish to investigate the magnification and resolution of such a lens. The impact of light scattering, chromatic aberration, and diffraction on resolution is explored theoretically and experimentally. The study presents theoretical analyses of the drop profile using thermodynamic principles and numerical methods. Ray tracing algorithms are employed to model light propagation through the system, considering refraction and reflection effects. Experimental validation of the theoretical models demonstrates strong agreement.

INTRODUCTION

This study explores the magnification and resolution capabilities of an imaging system employing a water droplet positioned on a glass surface. Through qualitative ray tracing and experimental investigation, the system's magnification is observed, with a focus on factors influencing resolution. The study examines the effects of light scattering, chromatic aberration, and diffraction on resolution both theoretically and experimentally. Experimental, the study utilized a DSLR camera, grids and Dirac delta functions for measurement and control of camera properties and environmental conditions. Furthermore, the study presents theoretical analyses of the drop profile using principles of thermodynamics and numerical techniques in Python. Ray tracing algorithms are utilized to simulate light propagation through the system, accounting for refraction and reflection phenomena. Experimental findings are compared against theoretical predictions, showing strong alignment. The study concludes by discussing variations in magnification and changes in resolution due to drop position and alignment. In summary, this investigation offers a comprehensive understanding of the imaging capabilities and constraints associated with water droplet-based lenses.

PHENOMENON

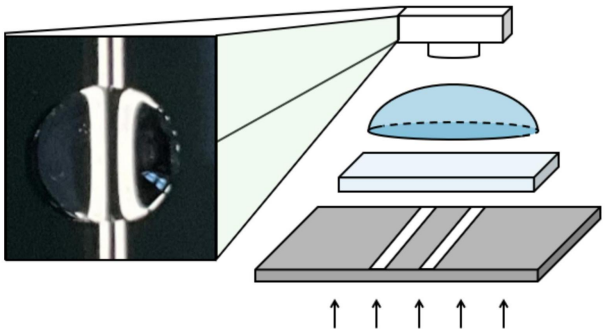

Figure 1: Schematic of Basic Theoretical Experimental Setup with an Example of Preliminary Experimental Results

In an imaging system consisting of a camera, a water drop, a slide of glass and a target, we observe that in the image captured by the camera, the target is being magnified by the drop class system. Qualitatively, looking at our imaging system from the side with our target object below, we can trace light rays up through the imaging system from the side, with our target object below. In tracing these light rays up through the imaging system, and due to a difference in the refractive indices in the water and air, rays are refracted away from the normal per Snell's Law, which is given by

$$n_1 \sin\theta_1 = n_2 \sin\theta_2$$

Where θ_1 and θ_2 are the angles of incidence and refraction, respectively, and n_1 and n_2 are the indices of refraction of water and air, respectively.

Performing qualitative ray tracing on our basic theoretical imaging system, we observe the magnification as expected by our preliminary experimental

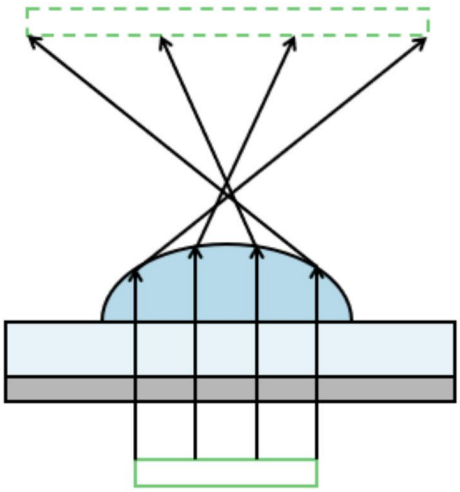

Figure 2: Ray Tracing to Demonstrate Magnification of Optical System

The magnification of our optical system is defined by the ratio between the lengths of our magnified image and object. However, when the target object is magnified the output image is not always sharp, and a magnified point results in a lower resolution airy disk. This change in resolution is caused by three

primary factors. First, the scattering of light rays due to small particles, such as salts or other minerals in our water droplet. Small particles scatter light of a shorter wavelength, while larger particles scatter light of a longer wavelength. Second, the difference in refractive indices of different wavelengths of light, which results in different wavelengths refracting at different angles, resulting in a phenomenon known as chromatic aberration, and third, the diffraction of light through the aperture of our camera.

Figure 3: Experimental and Theoretical Demonstration of Chromatic Abberation.

To quantify resolution, we will image pairs of lines and find the smallest line pair spacing that can be distinguished. This can either quantify this as spatial frequency in line pairs per mm, or find the angular frequency, a quantity that is independent of the zoom of our image by finding the lines per picture width to take into account the field of view of our camera, given by:

$$\xi = \frac{\text{Pixels Per Picture Width}}{\text{Pixels Per Line Pair}}$$

The second factor that impacts our ability to distinguish a line pair will also depend on the contrast of our photos taken as well as our resolution. When given a sinusoidal intensity profile, of the form

$$\text{Input}(\theta) = A_{\text{in}}\ \sin(2\pi\xi\theta)$$

our output image, which will be of the form

$$\text{Output}\ (\theta) = A_{\text{out}}\ \sin(2\pi\xi\theta)$$

will have a lower contrast. To explore the effects of resolution and contrast, we will find the modulation transfer function of our optical system defined as the ratio of output to input intensity amplitude given a certain angular frequency.

$$\text{MTF}(\xi) = \frac{A_{\text{out}}}{A_{\text{in}}}$$

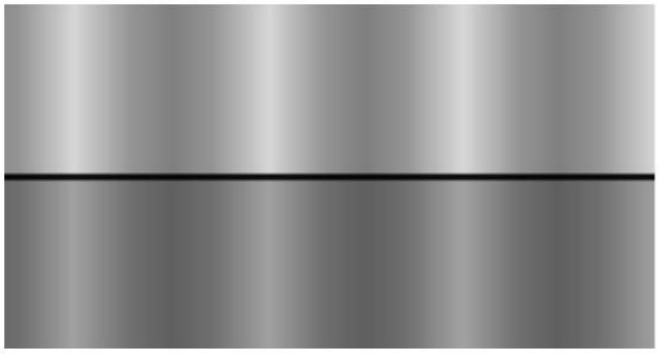

Figure 4: Visualization of Effect of Droplet on Sinusoidal Target. The top represents the original target, while the bottom represents the target after the light has travelled through the lens, where there has been a visible change in both resolution and contrast [2].

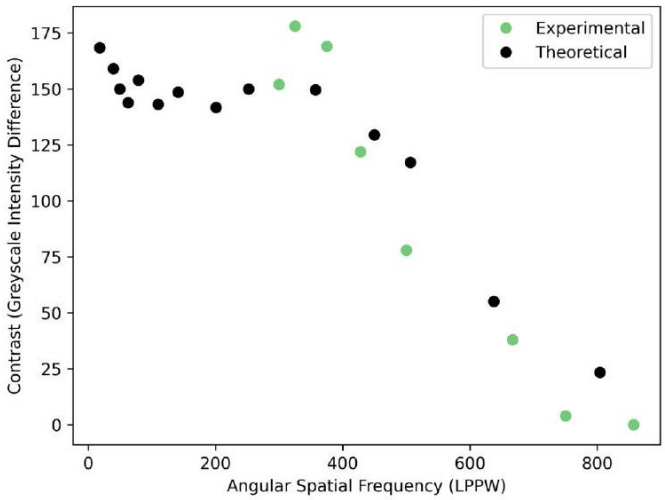

Figure 5: MTF vs. Angular Spacial Frequency obtained through Simulation and Experiment

EXPERIMENTAL DETAILS

Experimentally, a Nikon D3500 DSLR camera was mounted on a tripod on top to get a top view of the drop, while oriented sideways to obtain side profiles of the drop. The DSLR camera consists of a single lens with a sensor that reads an inverted image. Our FStop value was large (F18), in order to achieve a small aperture which allows less light in and therefore increases the depth of field, allowing the full image to be in focus as the picture can be taken from further away, where our lens has better focusing abilities. We used a smaller iso (ISO 100-400) for less noise and to minimize exposure. Finally, we used a slow shutter speed (1/30) to allow for better contrast. The droplet was placed on top of a glass slide coated with hydrophobic spray. A lamp was used to light the image from underneath, with no other top

or side sources of light in the surroundings to prevent reflections on the top of the surface of the drop. Additionally, a sheet of white paper was used in between the lamp and the glass slide to prevent the light from being aimed directly at the camera and causing reflections on the surface of the camera lens.

Figure 6: Experimental Setup Top View.

Figure 7: Experimental Setup Side View

Our targets consisted of grids to measure the magnification and Dirac delta intensity profiles, created by printing a 1-pixel thin line on a laser printer. We take measurements at varying angular spatial frequencies and construct intensity profiles at various spatial frequencies by taking the spacial fast fourier transform of the resulting intensity profile and dividing this by the constant FFT given by the original Dirac Delta function.

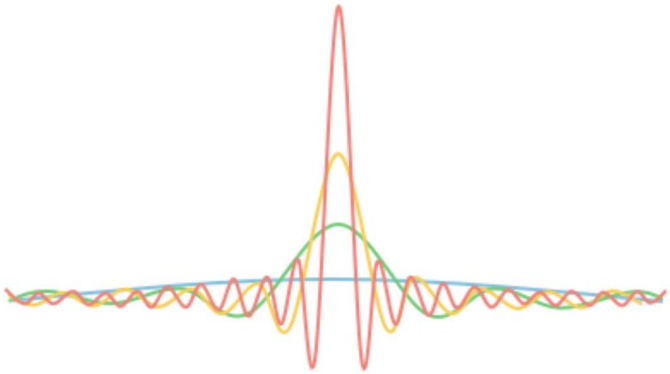

Figure 6: Dirac Delta Function is the Sum of Every Frequency, Resulting in a Constant FFT

THEORY

Drop Profile

For a 3d sessile drop we seek to minimize its thermodynamic potential

$$G = G_b + G_i + G_g$$

which consists of G_b, the thermodynamic contribution from the bulk of the drop which is constant for a given volume and temperature, G_i the net contribution of surface energies from the interfaces

$$G_i = \gamma_{lv} A_{lv} + \gamma_{sv} A_{sv} + \gamma_{ls} A_{ls}$$

and the gravitational potential energy / which can be found by integrating over the volume of the drop

$$G_g = \rho g \int_V \hat{y} \cdot \vec{r}(x, y, z) dV$$

This sum now becomes a functional we must minimize with the Lagrangian being the integrand.

$$G_i + G_g = \pi \left(\gamma_{lv} + \lambda_l\right) r^2 \left(\frac{\pi}{2}\right) + \pi \int_0^{\pi/2} \left(2\gamma_{lv} r \sqrt{\dot{r}^2 + r^2} + \frac{\rho g}{2} r^4 \cos\theta\right)$$

We can find the function r to minimize this functional by using the euler lagrange equation and imposing a volume constraint.

$$\frac{\partial \mathcal{L}}{\partial r} - \frac{\mathrm{d}}{\mathrm{d}\theta}\left(\frac{\partial \mathcal{L}}{\partial \dot{r}}\right) - \eta \frac{\partial f}{\partial r} = 0$$

Where

$$V = \frac{2\pi}{3}\int_0^{\pi/2} r^3 \sin\theta d\theta$$

The Lagrange multiplier physically represents the minimum pressure required to maintain this volume; that is a sessile drop must have constant pressure everywhere within the drop, so the radius of curvature must decrease for increasing height.

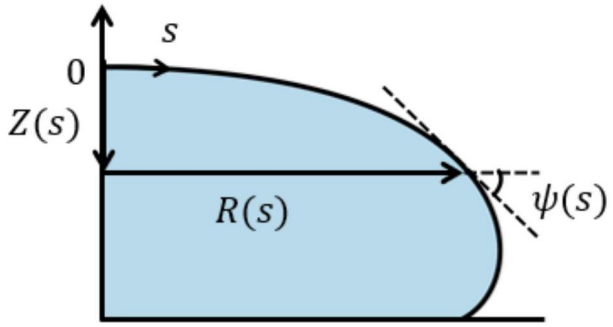

Figure 7: Defined Geometry of Drop Profile

We can now numerically solve in order to obtain the shape of the drop profile. Applying a coordinate transform now parametrized by arc length s, we can rewrite the resulting ordinary differential equation as follows:

$$\eta + \frac{\rho g}{\gamma_{lv}} Z\left(s_f\right) = \frac{\rho g}{\gamma_{lv}} Z(s) - \frac{\mathrm{d}\psi}{\mathrm{d}s} - \frac{\sin\psi}{R}$$

[1]

Where the value $\eta + \frac{\rho g}{\gamma_{lv}} Z\left(s_f\right)$ is constant for a given volume of the drop. Geometrically, two more first order ordinary differential equations can be obtained

$$\frac{\mathrm{d}R}{\mathrm{d}s} = \cos\psi \quad \frac{\mathrm{d}Z}{\mathrm{d}s} = \sin\psi$$

As well as the following initial conditions

$$R(0) = 0$$
$$Z(0) = 0$$
$$\psi(0) = 0$$

Additionally, the contact angle can be found with the following known equation.

$$\psi\left(s_f\right) = \cos^{-1}\left(\frac{\gamma_{sv} - \gamma_{ls}}{\gamma_{lv}}\right)$$

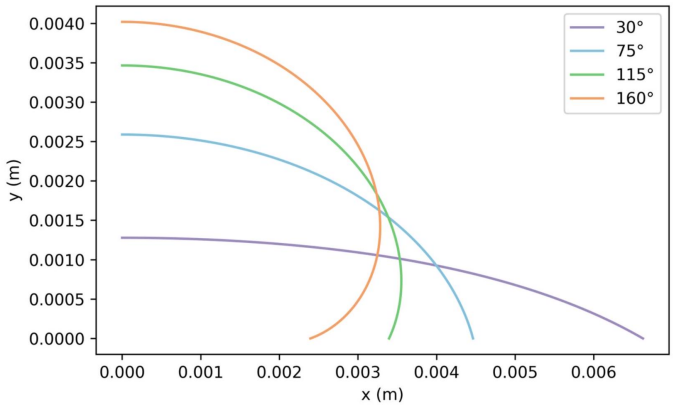

Figure 8: Solution to System of 3 First Order ODEs provided for a 100 Microliter Drop at Various Contact Angles.

To verify our drop profile experimentally, we place our droplet perpendicular to our DSLR camera, which is mounted on a tripod so that our camera can be adjusted until it is level with the drop. We obtain an image of the drop as well as a calibration stick, then used a tracking software to obtain numerical points along our drop profile.

Figure 9: Sample Experimental Picture and Experimental Setup for Determination of Drop Side Profile.

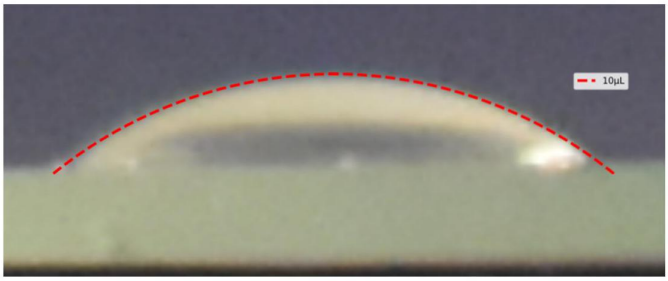

Figure 10: Experimental Correlation Between Numerical Solution and Experimental Droplet.

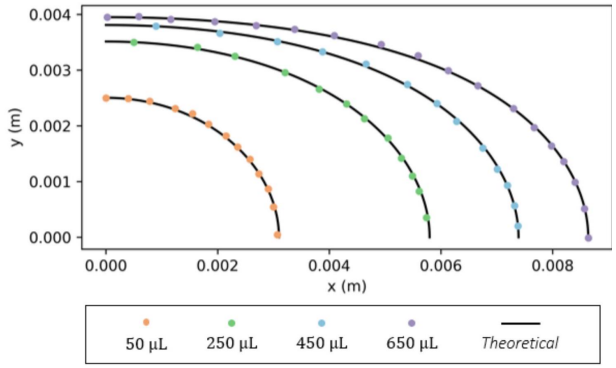

Figure 11: Strong Experimental Agreement Between Predicted and Simulated Droplet Profile for Various Volumes.

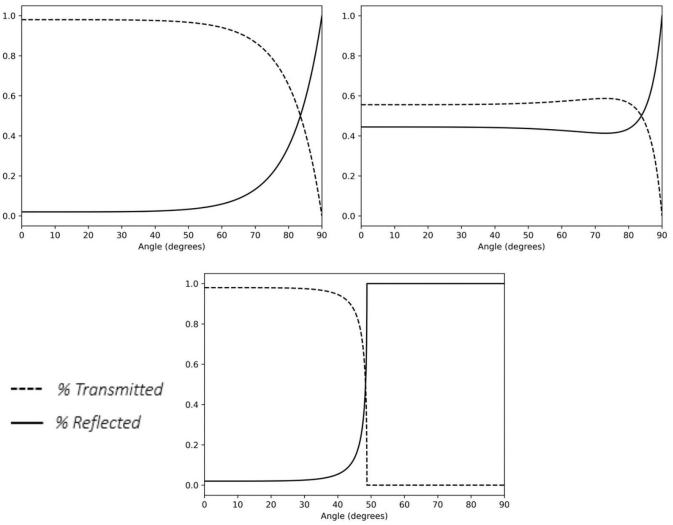

Figure 12: % Trasmitted vs. Reflected for $n_1 = 1, n_2 = 1.33$ and $n_2 = 5$ respectively. With a greater second index of refraction, we can see that more light is going to be reflected. For light travelling from a higher to a lower index of refraction ($n_1 = 1.33, n_2 = 1$), we see a critical angle at which total internal reflection occurs.

Ray Tracing

In order to introduce optics into our quantitative models, we will use a ray tracing algorithm, which traces rays from the camera through the image plane and to the droplet, initializing a vector for each ray that is refracted at each interface and eventually reaches the target plane. In reality, these rays travel the opposite direction, but we trace our rays backwards because we do not know which rays hit the camera in reality. For a given pixel on the image plane, the colour and intensity will depend on the colours on the target plane that the four rays passing through the corners hit as well as the area of the quadrilateral produced by these four rays.

$$n_1(\mathbf{i} \times \mathbf{n}) = n_2(\mathbf{t} \times \mathbf{n})$$

Additionally, we must account for the reflection of our rays. Our rays will reflect in the same direction we are propagating, with the amount of light reflected being an average of the reflected S and P polarized electromagnetic radiation which can be found with the Fresnel equations:

$$R_\perp(\theta_i) = \left(\frac{n_1 \cos\theta_i - n_2 \cos\theta_t}{n_1 \cos\theta_i + n_2 \cos\theta_t}\right)^2$$
$$R_\parallel(\theta_i) = \left(\frac{n_2 \cos\theta_i - n_1 \cos\theta_t}{n_2 \cos\theta_i + n_1 \cos\theta_t}\right)^2$$
$$R(\theta_i) = \frac{R_\perp(\theta_i) + R_\parallel(\theta_i)}{2}$$

We can write the ray that escapes the drop as all light that is not reflected:

$$T(\theta_i) = 1 - R(\theta_i)$$

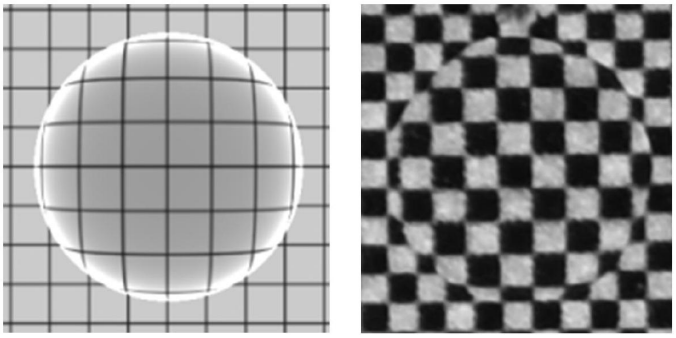

Figure 13: Theoretical vs. Experimental From Ray Tracing Algorithm for 25 Microliters.

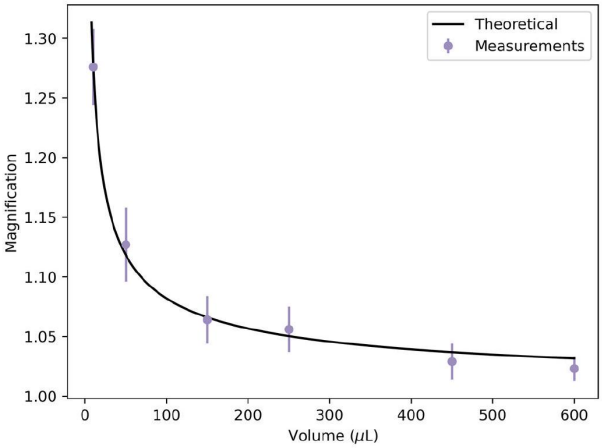

Figure 14: Comparison between Experimental Magnification at Center and Theoretical Magnification

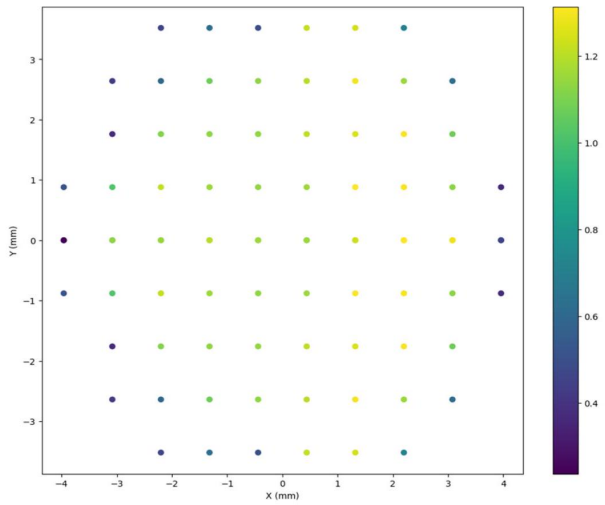

Figure 15: Magnification as a Function of Position of Drop when Camera is Intentionally Aligned Asymmetrically (Offset = 10 cm)

CONCLUSION

In conclusion, this study thoroughly investigates the magnification and resolution properties of an imaging system utilizing a single water droplet as a lens on a glass surface. Through a combination of theoretical analyses and experimental validation, we have gained insights into the behavior of light propagation, factors influencing resolution, and the structural dynamics of the droplet profile. Our investigation reveals that while the water droplet lens can indeed magnify images, the resulting output may not always exhibit optimal sharpness due to various factors such as light scattering, chromatic aberration, and diffraction. Theoretical models, supported by experimental data, provide a comprehensive understanding of these phenomena, enabling us to quantify resolution and explore its dependence on factors like contrast and spatial frequency.

Furthermore, our study delves into the theoretical underpinnings of droplet profile formation, employing thermodynamic principles and numerical methods to elucidate the drop's shape and behavior. Experimental validation demonstrates the efficacy of these theoretical models, showcasing strong agreement between predicted and observed droplet profiles. Ray tracing algorithms enable the modeling of light propagation through the system, allowing for a deeper understanding of refraction, reflection, and their impacts on imaging quality. The comparison between theoretical predictions and experimental results underscores the reliability and accuracy of our analytical approaches. In practical terms, the insights gained from this research can inform the design and optimization of imaging systems employing water droplet lenses, offering potential applications in fields ranging from microscopy to optical engineering.

[1] Jeffrey Bullard. Thermodynamics of sessile drops on a rigid substrate: A comparison of two theories, 2005-11-15 2005.
[2] Calvin Leung and T. D. Donnelly. Measuring the spatial resolution of an optical system in an undergraduate optics laboratory. *American Journal of Physics*, 85(6):429–438, 06 2017. ISSN 0002-9505. doi:10.1119/1.4979539. URL https://doi.org/10.1119/1.4979539.